
Low cost fabrication of PVA based personalised vascular phantoms for in vitro haemodynamic studies: three applications

Giacomo Annio[†]

Dept. Medical Physics and Bioengineering
University College London
Torrington Place WC1E 7JE London, UK
Email: giacomo.annio.15@ucl.ac.uk

Gaia Franzetti[†]

UCL Mechanical Engineering
University College London
Torrington Place
WC1E 7JE London, UK
Email: gaia.franzetti.15@ucl.ac.uk

Mirko Bonfanti

Wellcome/EPSRC Centre for
Interventional and Surgical Sciences
UCL Mechanical Engineering
University College London
Torrington Place WC1E 7JE London, UK
Email: m.bonfanti@ucl.ac.uk

Antonio Gallarelli

Dept. of Electronics, Information and Bioengineering
Politecnico di Milano
20133, Milano, Italy
Email: antonio.gallarelli@mail.polimi.it

Andrea Palombi

UCL Mechanical Engineering
University College London
Torrington Place
WC1E 7JE London, UK
Email: andrea.palombi.16@ucl.ac.uk

Elena De Momi

Dept. of Electronics, Information and Bioengineering
Politecnico di Milano
20133, Milano, Italy
Email: elena.demomi@polimi.it

Shervanthi Homer-Vanniasinkam

UCL Mechanical Engineering
University College London
Torrington Place
WC1E 7JE London, UK
Leeds Teaching Hospitals NHS Trust
Leeds, LS1 3EX, UK
Email: s.homer-v@ucl.ac.uk

Helge A. Wurdemann

UCL Mechanical Engineering
University College London
Torrington Place
WC1E 7JE London, UK
Email: h.wurdemann@ucl.ac.uk

Vanessa Díaz-Zuccarini

Wellcome/EPSRC Centre for
Interventional and Surgical Sciences
UCL Mechanical Engineering
University College London
Torrington Place WC1E 7JE London, UK
Email: v.diaz@ucl.ac.uk

Ryo Torii

UCL Mechanical Engineering
University College London
Torrington Place
WC1E 7JE London, UK
Email: r.torii@ucl.ac.uk

Stavroula Balabani^{*}

UCL Mechanical Engineering
University College London
Torrington Place
WC1E 7JE London, UK
Email: s.balabani@ucl.ac.uk

Gaetano Burriesci^{*}

Dept. Mechanical Engineering
University College London
Torrington Place
WC1E 7JE London, UK
Ri.MED Foundation
Via Bandiera, 11
90133, Palermo, Italy
Email: g.burriesci@ucl.ac.uk

Vascular phantoms mimicking human vessels are commonly used to perform in vitro haemodynamic studies for a number of bioengineering applications, such as medical device testing, clinical simulators and medical imaging research. Simplified geometries are useful to perform parametric studies, but accurate representations of the complexity of the in vivo system are essential in several applications as personalised features have been found to play a crucial role in the management and treatment of many vascular pathologies. Despite numerous studies employing vascular phantoms produced through different manufacturing techniques, an economically viable technique, able to generate large complex patient-specific vascular anatomies, still needs to be identified. In this work, a manufacturing framework to create personalised and complex phantoms with easily accessible and affordable materials is presented. In particular, 3D printing with polyvinyl alcohol (PVA) is employed to create the mould, and lost core casting is performed to create the physical model. The applicability and flexibility of the proposed fabrication protocol is demonstrated through three phantom case studies - an idealised aortic arch, a patient-specific aortic arch, and a patient-specific aortic dissection model. The phantoms were successfully manufactured in a rigid silicone, a compliant silicone and a rigid epoxy resin, respectively; using two different 3D printers and two casting techniques, without the need of specialist equipment.

1 Introduction

In the past 30 years, fluid dynamic investigations have played an important role in the study of the cardiovascular system, providing insight into disease condition and progression and support for management optimisation. *In vitro* haemodynamic studies typically rely on a physical representation - *synthetic phantom* - of the vessels of interest to replicate physiology or disease in the lab. Vascular phantoms have thus been successfully employed in numerous applications, ranging from the study of healthy and diseased haemodynamics in regions of the human cardiovascular system [1], to the assessment of the accuracy of imaging modalities and computational techniques [2], evaluation of medical devices [3] and the planning of surgical interventions [4]. Their success is due to the advances in medical imaging modalities and the commercialisation of 3D printing devices. The former provided access to higher resolution images and noise reduction in the acquired data, thus enabling the retrieval of 3D accurate geometries. The latter allowed the manufacturing of cost-efficient 3D models of regions of the circulatory system based on patient-specific data.

A broad range of vascular phantoms has been reported in the literature, varying in complexity depending on the study aims and assumptions made. Reported phantoms differ primarily in geometry, material properties and fabrication methods. In terms of geometry, vascular phantoms tend to vary from idealised to patient-specific ones. Even though idealised geometries can play a key role in parametric studies,

accurate anatomical descriptions are essential to reproduce patient-specific conditions and capture the *in vivo* haemodynamic features for a variety of applications; personalised features - morphology, flow patterns, pressures and velocities - have been shown to play an important role in several cardiovascular pathologies, and therefore diagnosis management and treatment are strictly patient-specific [5, 6]. Experimental mock circulatory loop that can reproduce individualised conditions are being developed in this context [7], alongside personalised computational models [8], that also necessitate fabrication of accurate vascular phantoms.

Vascular phantoms can be manufactured to be either rigid or compliant, in order to approximate the elastic properties of the vasculature. The choice of material often depends on the imaging modality employed for the *in vitro* study. For instance, rigid transparent models, manufactured mainly in resin [9] or glass [2], have commonly been employed in Particle Image Velocimetry (PIV) studies due to optical access requirements, whereas compliant models have often been manufactured using a broad range of opaque materials such as rubber-like compounds [10], silicone [11], latex [12] and polyurethane [13], which are compatible with magnetic resonance imaging (MRI).

Various phantom manufacturing methods have been reported in the literature. The most common ones are dipping [5], dripping [14], and the use of two different moulds, one for the inner and one for the outer part [15]. These approaches are invariably fraught with difficulties, especially when the geometry is complex. To overcome these challenges, soluble moulds made in materials such as wax [16] and isomaltose [17], that can be dissolved after the curing of the phantom material have been employed. These moulds can achieve fine detail, but the shrinkage occurring during the cooling process can lead to inaccuracies in the final model.

A comprehensive review of different manufacturing materials and procedures, and their limitations can be found in the work of Yazdi et al. [18]. It is apparent that despite the number of studies reported in the literature, manufacturing patient-specific phantoms in the laboratory at accessible cost and without the need of specialised equipment (e.g. big volume vacuum chambers, water jets) remains an issue, especially in the case of complex geometries and big volumes.

In this paper, we present a methodology to manufacture idealised and patient-specific vascular phantoms for haemodynamic studies and imaging applications in a low cost manner and without access to specialist equipment, addressing some of the limitations of previous works. In particular, negative moulds are created through 3D printing in polyvinyl alcohol (PVA), a water soluble material, to develop both compliant and rigid phantoms through a lost core casting process. The methodology and associated costs and equipment requirements are demonstrated through three aortic phantoms with different geometrical and mechanical properties; these include a simplified aortic arch, a patient-specific aortic arch and a patient-specific aortic dissection model.

*Corresponding authors. † The authors equally contributed to this work.

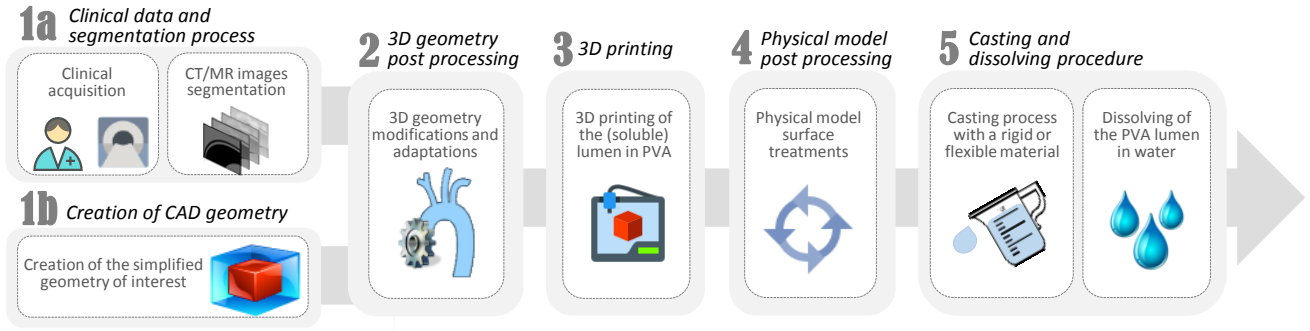


Fig. 1. The proposed PVA based manufacturing process: (1a) acquisition of patient-specific clinical images of the vessel of interest and segmentation process to reconstruct the geometry; (1b) creation of the CAD simplified geometry; (2) post-processing of the 3D geometry; (3) 3D printing of the vessel lumen in PVA; (4) Physical model refinement; (5) Casting and dissolving procedure of PVA in water

2 Material and Methods

In this section, the process of creating anatomical vascular phantoms using 3D printing in PVA is described.

2.1 Manufacturing process

The manufacturing process adopted in this study involves five stages, as illustrated in Fig. 1 and explained in detail in the following sections: (1) Creation of the geometry either via segmentation of patient-specific clinical images or creation of a CAD idealised geometry; (2) 3D post processing; (3) 3D printing in PVA; (4) Physical model refinement; (5) Casting and dissolving of PVA in water.

Clinical data and segmentation process

Volumetric medical images (e.g. computed tomography (CT), magnetic resonance imaging (MRI)) are used to reconstruct patient-specific vessels via the segmentation process. Image segmentation is the process of partitioning a digital image into different regions containing pixels with similar attributes. It is used to identify and label regions of interest and can be used to create volumetric reconstructions of different organs and tissues. For vascular phantoms, thresholding is commonly employed to reconstruct the lumen volume (i.e. blood volume). It uses the background to foreground contrast ratio to isolate the region of interest. Manual refinement is lastly used to adjust the vessel area, especially in the presence of complex anatomies. Details regarding the segmentation procedure and the mesh refinement can be found in Bücking et al. [19].

This first step is not necessary in the case of idealised geometries and the process starts with the generation of the CAD geometry (Step 1b in Fig. 1).

3D geometry post processing

The image segmentation process yields a 3D model of the target area. Smoothing of the surface is subsequently performed to compensate for errors resulting from the resolution of the original medical images and to facilitate the manufacturing of the building components. Geometrical modifications can be made in this stage according to the purpose of the vascular phantom. For instance, for use with *in vitro*

studies, inlet and outlet sections need to be designed to accommodate the phantom within the experimental system.

3D printing

The CAD model reconstructing the vessel lumen volume is 3D printed in PVA using a stereolithography (SLA) printer. PVA is commonly employed as a support material to create complex geometries in Polylactic acid (PLA), which is then dissolved in water to obtain the object of interest. However, in this work, it is used as the primary material to create a mould for the casting process (i.e. negative mould). Attention was paid to the choice of the infill, one of the most important factors for 3D printing (i.e. the structure printed inside the object). A higher infill will result in a stronger model, which is especially important in the case of a complex structure, but it will also lead to increased duration of the PVA dissolving process.

Physical model refinement

The 3D printed model, constituting the negative mould, undergoes further post processing before the casting procedure. In order to make the surface smoother, liquid PVA glue can be used to provide a good finish to the phantom thereby reducing surface roughness. A transparent acrylic spray paint (PlastiKote, UK or Humbrol, UK) is lastly used to make the contact surface impermeable and hydrophobic, so as to reduce chemical interactions with the casting material.

Casting and dissolving procedure

The final stage in the manufacturing process is the casting. In this phase, the physical phantom is created around the PVA model of the vessel lumen, which is then dissolved, resulting in the hollow structure. Two casting options are available, as illustrated in Fig. 2: (i) to enclose the model in a rigid box and pour the casting material to fill the space, which will result in a box with a hollow structure reproducing the vessel lumen; or (ii) to design an external mould according to the vessel geometry to control the vessel wall thickness. In this scenario, the casting material is poured in-between the two, resulting in a physical phantom having the shape of the

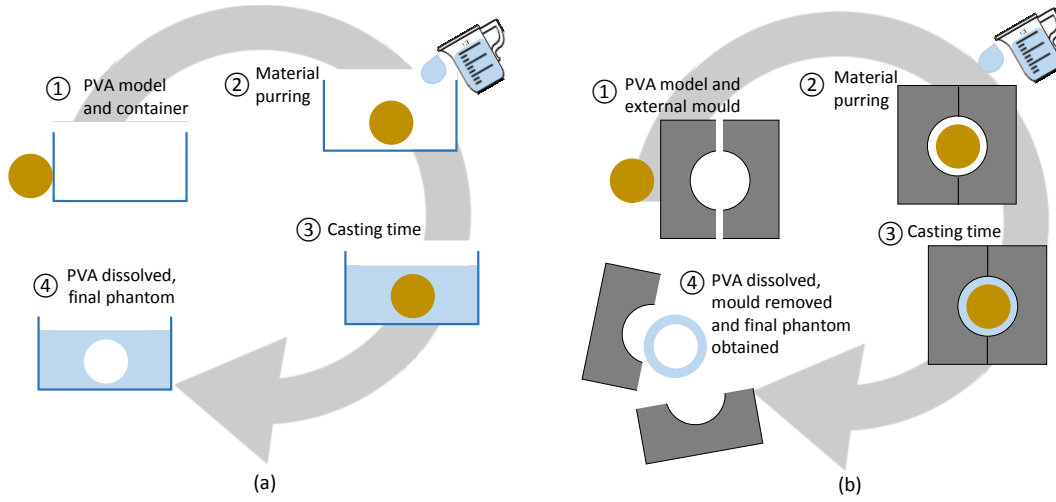


Fig. 2. Schematics of the two casting options: (a) enclosing the PVA model in a box and pour the casting material, which will result in a hollow structure once the material is dissolved; and (b) including a positive mould to control the wall thickness of the phantom. This will result in a physical model having the shape of the vessel of interest

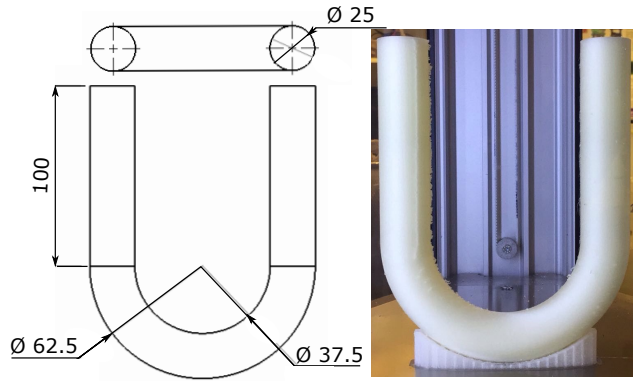


Fig. 3. Geometry and 3D printed PVA phantom of the simplified case-Phantom 1

vessel of interest.

The casting material can be selected based on the design criteria. For instance, paying particular attention to the mechanical properties (e.g. Young's modulus) in case of flexible phantoms or to the optical characteristics (e.g. transparency and Refractive Index, RI) for compatibility with the imaging modalities employed (e.g. PIV). The curing time is adjusted accordingly, and subsequently the object is placed in a water bath to let the inner PVA mould dissolve.

2.2 Phantom 1: Simplified aortic arch model

Phantom 1 was manufactured to reproduce a simplified aortic arch without branch vessels, realised as a U bend (Fig. 3). It was designed to be rigid and compatible with both MRI and PIV imaging, which necessitates the use of an optically transparent material. The mould was designed with a CAD software (SolidWorks, Dassault Systmes, Canada) and then 3D printed in PVA using a Delta WASP 2040 Turbo 2 (Wasp, Italy). For the casting process, an acrylic box with flat sides was manufactured to allow PIV laser illumination and pouring of the selected printing material; a clear, solvent free,

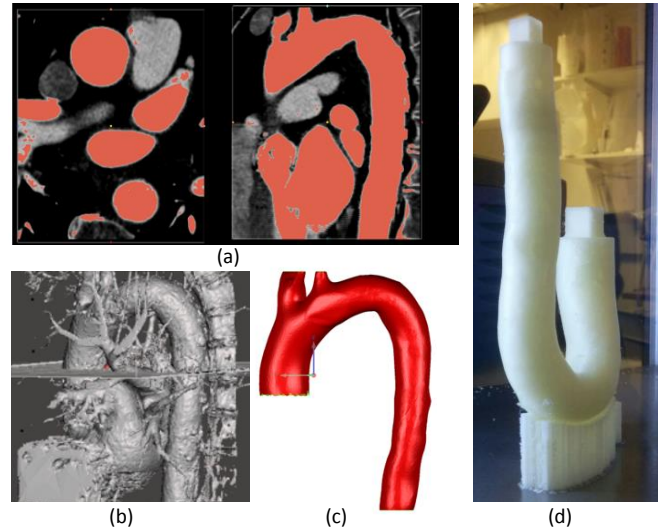


Fig. 4. Lumen of Phantom 2: (a) segmentation process, (b) 3D volumetric reconstruction, (c) geometry extraction and (d) PVA printed mould

low viscosity silicone elastomer (MED 6015, NuSil Technology, CA, USA) with a RI = 1.4. The entire model was immersed in water and the inner mould in PVA dissolved. The compatibility of Phantom 1 with PIV measurements was subsequently tested.

2.3 Phantom 2: Patient-specific aortic model

Phantom 2 was manufactured from patient-specific data and designed to be flexible, in order to mimic the compliant behaviour of the vessel. The original dataset was obtained from a CT angiography of a 76-year-old patient undergoing a TAVR (Transcatheter aortic valve replacement) procedure. The study was reviewed and approved by the internal review board of the research group, which was the relevant cross-institutional committee responsible for assessing the

methodological appropriateness and ethics of the study design (AO San Camillo-Forlanini, Rome, Italy). The subject gave written informed consent in accordance with the Declaration of Helsinki and the data set was anonymised. Segmentation was performed using 3DSlicer (Slicer, NIH) and part of the vessel ascending aorta, aortic arch and the initial part of the abdominal aorta - was reconstructed (Fig. 4c).

The structure was post-processed using Geomagic Control (3D Systems, Canada) and MeshMixer (Autodesk, USA). Smoothing was performed to reduce the noise introduced by the thresholding method, in order to prepare the surface to the 3D printing process. The aortic lumen volume was 3D printed in PVA with a Delta WASP 2040 Turbo 2 (Wasp, Italy) (Fig. 4d). Since Phantom 2 was designed to reproduce the vessel wall thickness and mimic its compliance, a second, external mould was printed. An offset value of 2 mm was applied to the 3D aortic geometry and three pins were added to the internal geometry to allow a stable alignment between the internal and external moulds, hence maintaining the correct gap. The outer part of the mould was separated in multiple sections in order to simplify the extraction process of the phantom. These parts were kept together by mean of bolts and nuts to guarantee a perfect alignment. The external mould was printed using white resin with a Form 2 3D printer (FormLabs, USA).

Silicone (Smooth-On Ecoflex 00-30 silicone) was selected as phantom material and casting was performed by pouring the material in between the two moulds, in order to reproduce the desired vessel wall thickness. Once cured, the external part was removed and the inner PVA model dissolved in water. For ease of connection to the experimental mock loop and to avoid any unwanted movement of the central part of the phantom, the latter was placed in a custom made box and the inlet and outlet connected to rigid connectors.

2.4 Phantom 3: Patient-specific diseased aortic model

Phantom 3 was created to illustrate the manufacturing process of a patient-specific case of a complex pathological vascular geometry, using Type-B Aortic Dissection as a case study. In this pathology, a tear in the aortic wall causes the creation of two separate lumina, the false (FL) and the true (TL) lumina, posing a major manufacturing challenge. Due to the relatively large dimensions of this geometry, it was essential in this case to minimise the costs and processing, by avoiding casting materials requiring degassing procedures (i.e. no equipment needed).

A patient was imaged with a CT scanner (Siemens AG, Munich, Germany; Field of View: 284 mm, slice thickness: 1 mm), thus obtaining 946 slices with an in plane resolution of 0.55 mm and inter-slice distance of 0.7 mm. The geometry of the aortic model was created (ethical approval study no 788/RADRES/16) with the software ScanIP (Synopsys, Mountain View, CA, USA) using a semi-automated segmentation tool based on thresholding operations. Smoothing was performed on the resulting masks to reduce the artefacts due to pixelation (Fig. 5). The final geometry file was exported

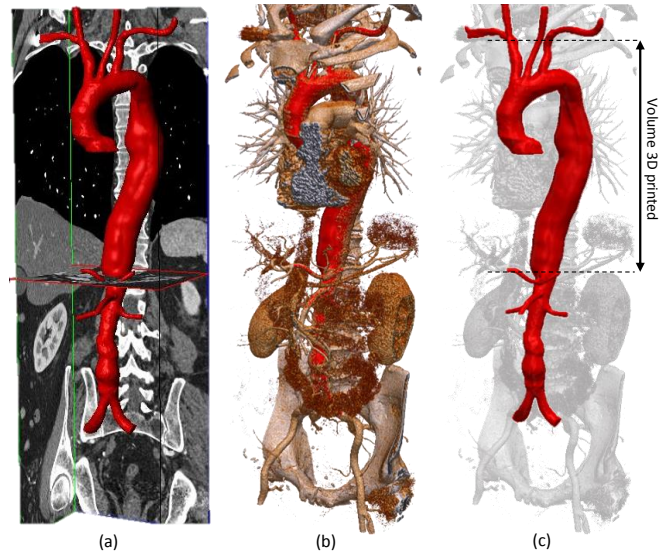


Fig. 5. Segmentation procedure and geometry extraction of Phantom 3: (a) segmentation process, (b) 3D volumetric reconstruction and (c) geometry extraction. In the picture is also highlighted the volume considered for the manufacturing of the physical model

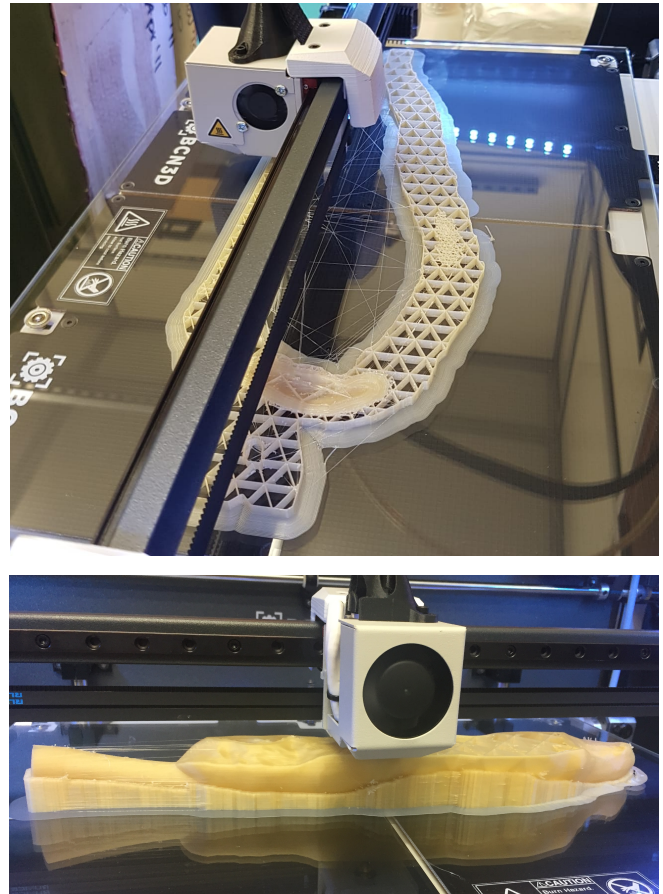


Fig. 6. 3D printing process of Phantom 3 in PVA. The geometry was printed with support material. in the picture it can be noted the geometry of the infill used

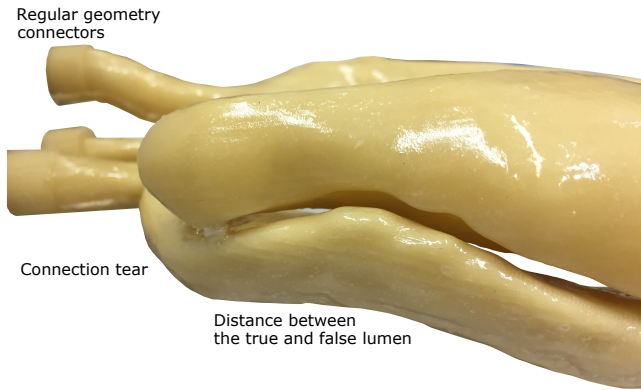


Fig. 7. Picture of the 3D PVA printed negative mould for Phantom 3 illustrating the complexity of the geometry, which includes the true and false lumen and a small connection tear in between. Connectors are added to the geometry to facilitate installation in the experimental rig

into a CAD software in order to modify the model for compatibility purposes with the experimental rig. In particular, rigid regular connectors were added to the geometry to facilitate the connection with the experimental rig. The stl file was created and the lumen region of both the TL and FL was 3D printed in PVA using a SigmaX printer (BCN3D, Spain). To avoid problems during the printing phase and reduce the support material needed, the TL and FL were printed separately and connected later in the post processing phase (Fig. 6).

The physical model was post-processed in three steps. First, several coats of PVA liquid glue were added on the external surfaces to reduce the roughness due to the different printing layers. Second, the TL and FL were joined together employing the same dissoluble glue guided by the connecting tear. Third, a transparent spray acrylic paint was used to make the surface impermeable and hydrophobic. This was also performed to avoid possible absorption of the PVA from the casting material.

Similarly to Phantom 1, a custom made box was designed and manufactured in polypropylene to contain the model and allow the casting process. Particular attention was made to align the inlet and outlets of the geometry to avoid any misalignment between the TL and FL. A rigid clear epoxy resin (GlassCast 50, EasyComposites, UK) was used as casting material, selected to minimise cost and bypass the need for degassing. Different layers of up to 50 mm were poured sequentially to avoid possible exothermic reactions during the curing process. At the end of the curing phase, the external polypropylene box was mechanically removed and PVA dissolved in warm water.

3 Results and Discussion

Table 1 summarises the technical properties of the three different phantoms manufactured in this work, including material costs and necessary equipment.

Two different 3D printers were used and both allowed the creation of a detailed and accurate geometry of the vessel

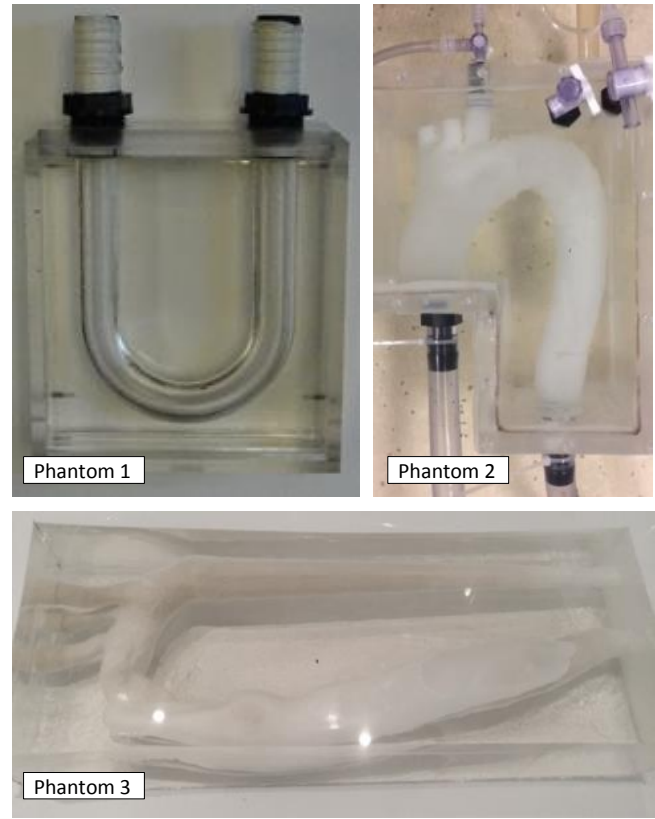


Fig. 8. Pictures of the three phantoms manufactured in this work

lumen. In particular, Fig. 7 shows the details of the complex curvature of the lumen for the pathological aorta reconstructed in Phantom 3 illustrating the ability of the printer to follow the intricacy of the structure. The infill chosen (i.e. 30%) was a good compromise between model strength and ease of dissolution for all the phantoms produced. To further facilitate this process, lower values can be chosen when the geometry is simplified or has a small volume, as for Phantoms 1 and 2.

The post-processing of the 3D printed physical model with PVA liquid glue was necessary to smoothen the surface and reduce the roughness due to the printing process. Equally important was the acrylic spray treatment to avoid the interaction between the casting material and the PVA, which would have resulted in opaque/ slightly coloured final cast model. This aspect was of utmost importance for Phantom 1, designed to be optically clear, and compatible with PIV measurements.

Casting was performed within 2 days of the printing of the model and the three materials used did not show any interaction with PVA. For both the rigid phantoms, successive layers were poured during the casting process. For Phantom 1 this was necessary to minimise the layer thickness in order to avoid air bubbles remaining trapped in the material after the degassing procedure, whereas for Phantom 3 due to a specific layer thickness limit imposed to minimise the exothermic reaction of the resin. This aspect may represent a limitation in specific applications, due to the layers becoming distinguishable. For instance, in the case of PIV experiments,

Table 1. Technical specifications and comparison of key manufacturing features among the three phantoms

	Phantom 1	Phantom 2	Phantom 3
Geometry	Simplified aortic arch	Patient-specific aortic arch	Patient-specific diseased aorta
Material	Rigid	Compliant	Rigid
Segmentation	/	3D Slicer	ScanIP
3D printer	Delta Wasp 2040 Turbo 2	Delta Wasp 2040 Turbo 2	BCN3D Sigmax
3D printing material	Formfutura PVA 1.75 mm	Formfutura PVA 1.75 mm	PVA eSun 2.85 mm
3D filament cost	\$45 / 300g	\$45 / 300g	\$38 / 500g
Casting material	Nusil MED 6015	Smooth-On Ecoflex 00-30 silicon	Epoxy resin
Casting material cost	\$154 / pint	\$19 / phantom	\$89 / 5Kg
Other equipment needed	Small vacuum chamber	External mould (\$254)	None
PIV compatibility	Yes (RI=1.4)	No	No
MRI compatibility	Yes	Yes	Yes

the layers used in the casting sequence may pose a challenge in illuminating different planes in the flow; in order to overcome this limitation, in the present study extra care was taken to align the casting layers with the PIV imaging planes.

Comparing the two rigid materials, Nusil MED 6015 was proved to be a good choice to reproduce PIV compatible phantoms with a contained volume (because of the higher cost of the material) and when a degassing chamber is available. On the contrary, the use of an epoxy resin allowed to overcome the degassing procedure, reducing the costs and making it suitable for large geometries eliminating the need for access to specialist equipment.

Finally, for all phantoms the dissolving of PVA was facilitated using warm and pressurised water. The duration of this process was directly related to the complexity of the geometry, from approximately 1 day for Phantom 1 to 3 days for Phantom 3. This phase was also facilitated by mechanical friction inside the phantoms (e.g. using a thin plastic rod), exercising care not to scratch the inner surface of the model.

Regarding imaging modalities, all the three phantoms were MRI compatible but, due to higher requirements, only Phantom 1 was compatible with PIV. Refractive index matching with the chosen material was successfully realised using a water-glycerol mixture (RI = 1.4) as working fluid in the experiments.

4 Conclusions

Manufacturing of physical phantoms to reproduce vessel geometries is essential to perform *in vitro* haemodynamic studies of the vascular system, test medical devices and surgical procedures, validate computational models and imaging modalities, as well as serve as training tools. Despite the numerous studies described in the literature regarding different phantoms and manufacturing modalities, costs and necessary equipment still present a limitation.

In this work, a combination of affordable and accessible methodologies and materials is described for three different case studies of increasing complexity: an idealised aortic arch, a patient-specific aortic arch and a patient-specific diseased aorta. In particular, 3D printing with water-dissolvable PVA was employed to create the vessel mould and casting was performed to create the final physical model. The three cases vary in geometrical complexity and volume dimensions, material mechanical properties (i.e. rigid or flexible), costs involved, equipment needed and imaging modalities compatibility. In particular, three different model materials, two casting procedures and two 3D printers were compared.

The described approaches represent cost-effective and highly affordable options to create physical vascular phantoms. Moreover, the case studies showcased a range of possibilities according to different design requirements, demonstrating the flexibility of the adopted methodologies.

Acknowledgements

Financial support by BHF (grant agreement no. FS/15/22/31356), EPSRC (grant agreement no. EP/L016478/1, EP/N509577/1 and EP/S014039/1), and the Springboard Award of the Academy of Medical Sciences (grant agreement no. SBF003-1109) is gratefully acknowledged. The authors are thankful to Mr. Gabriele Maritati and Ms. Sapna Puppala for providing the clinical data used in this work as well as the consenting patients.

References

- [1] Botnar, R., Rappitsch, G., Beat Scheidegger, M., Liepsch, D., Perktold, K., and Boesiger, P., 2000. "Hemodynamics in the carotid artery bifurcation:". *Journal of Biomechanics*, **33**(2), pp. 137–144.
- [2] van Ooij, P., Guédon, A., Poelma, C., Schneiders, J., Rutten, M. C. M., Marquering, H. A., Majoie, C. B.,

- van Bavel, E., and Nederveen, A. J., 2012. "Complex flow patterns in a real-size intracranial aneurysm phantom: Phase contrast MRI compared with particle image velocimetry and computational fluid dynamics". *NMR in Biomedicine*, **25**(1), pp. 14–26.
- [3] Carey, R. F., Herman, B. A., Robinson, R. A., Stewart, H. F., Hoops, R. G., & Douglas, G. H., 1991. U.S. Patent No. 5,052,934.
- [4] Russ, M., OHara, R., Setlur Nagesh, S. V., Mokin, M., Jimenez, C., Siddiqui, A., Bednarek, D., Rudin, S., and Ionita, C., 2015. "Treatment Planning for Image-Guided Neuro-Vascular Interventions Using Patient-Specific 3D Printed Phantoms". pp. 219–227.
- [5] Rudenick, P. A., Bijmens, B. H., García-Dorado, D., and Evangelista, A., 2013. "An in vitro phantom study on the influence of tear size and configuration on the hemodynamics of the lumina in chronic type B aortic dissections". *Journal of Vascular Surgery*, **57**(2), pp. 464–474.e5.
- [6] Bonfanti, M., Balabani, S., Greenwood, J. P., Puppala, S., Homer-Vanniasinkam, S., and Díaz-Zuccarini, V., 2017. "Computational tools for clinical support: a multi-scale compliant model for haemodynamic simulations in an aortic dissection based on multi-modal imaging data". *Journal of the Royal Society, Interface*, **14**(136), p. 20170632.
- [7] Franzetti, G., Diaz-Zuccarini, V., and Balabani, S., 2019. "Design of an in vitro mock circulatory loop to reproduce patient-specific vascular conditions: towards precision medicine". *To appear in: Journal of Engineering and Science in Medical Diagnostics and Therapy*.
- [8] Bonfanti, M., Franzetti, G., Maritati, G., Homer-Vanniasinkam, S., Balabani, S., and Diaz-zuccarini, V., 2019. "Patient-specific haemodynamic simulations of complex aortic dissections informed by commonly available clinical datasets". *To appear in: Medical Engineering & Physics*.
- [9] de Zélicourt, D., Kitajima, H., Yoganathan, A. P., Frakes, D., and Pekkan, K., 2005. "Single-Step Stereolithography of Complex Anatomical Models for Optical Flow Measurements". *Journal of Biomechanical Engineering*, **127**(1), p. 204.
- [10] Biglino, G., Verschueren, P., Zegels, R., Taylor, A. M., and Schievano, S., 2013. "Rapid prototyping compliant arterial phantoms for in-vitro studies and device testing.". *Journal of cardiovascular magnetic resonance : official journal of the Society for Cardiovascular Magnetic Resonance*, **15**(1), p. 2.
- [11] Tango, A. M., Salmons-Smith, J., Ducci, A., and Burriesci, G., 2018. "Validation and Extension of a FluidStructure Interaction Model of the Healthy Aortic Valve". *Cardiovascular Engineering and Technology*, **9**(4), pp. 739–751.
- [12] Tyszka, J. M., Laidlaw, D. H., and Asa, J. W., 2000. "Three-dimensional, time-resolved (4D) relative pressure mapping using magnetic resonance imaging - Tyszka - 2000 - Journal of Magnetic Resonance Imaging - Wiley Online Library". *Journal of Magnetic Resonance Imaging*, **329**, pp. 321–329.
- [13] Tai, N. R., Salacinski, H. J., Edwards, A., Hamilton, G., and Seifalian, A. M., 2000. "Compliance properties of conduits used in vascular reconstruction". *British Journal of Surgery*, **87**(11), pp. 1516–1524.
- [14] Tanné, D., Bertrand, E., Kadem, L., Pibarot, P., and Rieu, R., 2010. "Assessment of left heart and pulmonary circulation flow dynamics by a new pulsed mock circulatory system". *Experiments in Fluids*, **48**(5), pp. 837–850.
- [15] Cao, P., Duhamel, Y., Olympe, G., Ramond, B., and Langevin, F., 2013. "A new production method of elastic silicone carotid phantom based on MRI acquisition using rapid prototyping technique". In Proceedings of the Annual International Conference of the IEEE Engineering in Medicine and Biology Society, EMBS, IEEE, pp. 5331–5334.
- [16] Shmueli, K., Thomas, D. L., and Ordidge, R. J., 2007. "Design, construction and evaluation of an anthropomorphic head phantom with realistic susceptibility artifacts". *Journal of Magnetic Resonance Imaging*, **26**(1), pp. 202–207.
- [17] Allard, L., Soulez, G., Chayer, B., Treyve, F., Qin, Z., and Cloutier, G., 2009. "Multimodality vascular imaging phantoms: A new material for the fabrication of realistic 3D vessel geometries". *Medical Physics*, **36**(8), pp. 3758–3763.
- [18] Yazdi, S. G., Geoghegan, P. H. ., Docherty, P. D., Jermy, M. ., and Khanafer, A. ., 2018. "A Review of Arterial Phantom Fabrication Methods for Flow Measurement Using PIV Techniques". *Annals of Biomedical Engineering*, **46**(11), pp. 1697–1721.
- [19] Bücking, T., Hill, E., Robertson, J., Maneas, E., Plumb, A., and Nikitichev, D., 2017. "From medical imaging data to 3D printed anatomical models". *PLoS ONE*, **12**(5), pp. 1–10.